Published in final edited form as:
J Neurosci. 2008 August 13; 28(33): 8150–8160. doi:10.1523/JNEUROSCI.1744-08.2008.

Developmental Control of Synaptic Receptivity

Alison J. Barker[1], **Selina M. Koch**[1,2], **Jamian Reed**[1], **Ben A. Barres**[3], and **Erik M. Ullian**[1,2]

1*University of California, San Francisco Dept Ophthalmology & Physiology 10 Koret Way San Francisco, CA 94143-0730*

2*Neuroscience Graduate Program, University of California, San Francisco*

3*Stanford University School of Medicine Department of Neurobiology Fairchild Science Building D235 Stanford, CA 94305-5125*

Abstract

Are neurons born with the ability to form and receive synapses or do they acquire these abilities during development? We have previously found that purified postnatal retinal ganglion cells (RGCs) require soluble astrocyte-derived signals to form synapses *in vitro* and *in vivo*. Here we show that newly-generated embryonic day 17 (E17) RGCs are able to form but not receive synapses under these conditions. Dendrite growth is not sufficient to trigger receptivity; rather the ability of newly-generated RGCs to receive synapses is acquired at embryonic day 19 (E19) in response to direct contact by neighboring cell types. Direct contact with astrocytes, which are not present at E17 but are normally generated by E19, is sufficient to induce synaptic receptivity in E17 RGCs. In contrast, amacrine contact does not induce synaptic receptivity. Interestingly, astrocyte contact alters the localization of the synaptic adhesion molecule, neurexin, away from dendrites. In addition, dendritic expression of neurexin is sufficient to prevent astrocyte contact-mediated increases in synapse number, suggesting a molecular mechanism by which astrocyte contact regulates neuronal synaptic receptivity. Thus, synaptic receptivity is not induced simply by dendritic elaboration but must be signaled by both contact-mediated signaling from astrocytes and a shift in the dendritic localization of neurexin.

Keywords

synaptogenesis; Retinal Ganglion Cells (RGCs); astrocytes; glia; dendrite arbourization; rat

Introduction

Significant advances have been made in our understanding of the molecular mechanisms of synaptogenesis; yet we still understand little about how the number of synapses a neuron makes or receives is regulated both temporally and spatially. For example, is synapse number an intrinsic property of a neuron or is it largely controlled by extrinsic signals? And, when do embryonic neurons turn on their developmental program or become receptive to extrinsic signals? Recent studies of purified neurons show that synapse number can be controlled by extrinsic signals. RGCs purified away from all other retinal cell types are unable to effectively form synapses unless co-cultured with astrocytes, which provide soluble signals such as thrombospondin, that strongly enhance the number of synapses these neurons can make (Nagler et al., 2001; Mauch et al., 2001; Ullian et al., 2001; Christopherson et al., 2005). Similarly,

Correspondence to: Erik M. Ullian University of California, San Francisco, Dept Ophthalmology, 10 Koret Way, San Francisco, CA 94143-0730, ulliane@vision.ucsf.edu.

purified spinal motor neurons also depend on extrinsic signals provided by astrocytes or Schwann cells to form synapses *in vitro* (Ullian et al, 2004a). These studies provide evidence that extracellular signals from non-neuronal cell types can powerfully control synaptogenesis and raise the question of whether newly generated neurons are intrinsically capable of synaptogenesis. The possibility that either intrinsic or extrinsic developmental programs help to regulate the timing, location, or number of newly forming synapses has received relatively little consideration.

Though it is generally assumed that neurons are generated with the ability to both form and receive synapses, an earlier study found embryonic hippocampal neurons are capable of forming but not receiving synapses. These cultured embryonic neurons acquire synaptic receptivity at the same time that their dendritic arbors begin to elaborate. While the timing of these events suggests that synaptic receptivity is controlled by the amount of dendritic area available to receive synaptic inputs (Fletcher et al., 1994), it does not preclude the possibility that there are two distinct mechanisms, one controlling dendrite elaboration and a second controlling synaptic receptivity.

Here we have taken advantage of our methods to highly purify and culture rodent retinal ganglion cells (> 99% purity) to investigate when and how synaptic receptivity is acquired during normal development. RGCs purified from embryonic day 17 (E17) are unable to receive many synapses, even when they have extended long dendrites, and even though they are able to form synapses on more mature postnatal RGCs. Purified E17 RGCs do not acquire the ability to receive synapses with time in culture indicating that synaptic receptivity is not acquired as the result of an intrinsic maturation program. RGCs in mixed retinal cultures or *in vivo* are fully able to receive synapses at embryonic day (E) 19. Significantly E19 marks the first contacts between RGCs and various retinal cell types, strongly indicating that synaptic receptivity is induced by neighboring cell types.

Because RGCs establish contact with amacrine cells and astrocytes during embryonic development, we tested the hypothesis that contact with these cells is responsible for initiating synaptic receptivity. Co-culture of purified E17 RGCs in contact with purified astrocytes, but not with purified amacrine cells, is sufficient to induce synaptic receptivity. These findings show that developing RGCs are not born with the ability to receive synapses, but acquire it in response to contact-mediated signaling by neighboring cells.

Additionally we report that concomitant with the induction of embryonic synaptic receptivity, astrocyte contact induces changes in the dendrite localization of the synaptic protein neurexin. In mammals three neurexin genes have been identified each with an α and shortened β form (Dean & Dresbach, 2006; Craig & Kang, 2007). While neurexin is traditionally viewed as the pre-synaptic component of the neurexin-neuroligin complex, recent evidence (Taniguchi et al. 2007) has shown endogenous levels of dendritic neurexin. Interestingly this endogenous expression is postulated to play an inhibitory role in synapse formation. We have found that embryonic neurons have significant neurexin localization to dendrites and this localization is reversed by astrocyte contact, providing a possible mechanism by which developing neurons regulate the precise timing of synapse formation in response to contact with neighboring cell types. Importantly we were able to show that overexpression of a single neurexin, neurexin1β eliminated the astrocyte contact effect, providing support for an inhibitory role for neurexin in synapse formation.

Materials and Methods

Cell purification and culture

Step-by-step protocols for all procedures are available by request to barres@stanford.edu. RGCs from postnatal day 5 (P5) or embryonic day 17 (E17) albino rats (Simonson rats, Simonson Labs; Gilroy, CA) were purified as previously described (Barres et al., 1988). Briefly, dissected retinas were enzymatically dissociated in papain in Dulbecco's Phosphate Buffered Saline (Gibco; Carlsbad, CA) to create a single-cell suspension. RGCs were isolated from this suspension using sequential immunopanning to greater than 99.5% purity (Barres et al., 1988). Purified RGCs were plated on 12mm glass coverslips (Carolina Science and Math; Burlington, NC) in 24-well tissue culture plates (BD Biosciences; San Jose, CA) at a density of 30,000 cells per coverslip (Approximately 26,000 cells / cm^2). Coverslips were pre-treated for thirty minutes with poly-D-lysine (PDL; 70kDa, 10μg/mL; Sigma; St. Louis, MO) at room temperature followed by overnight incubation with mouse laminin (Sigma; St. Louis, MO).

RGCs were cultured in 500μL of defined, serum-free medium, modified from Bottenstein (1979). Media contained Neurobasal (Gibco; Carlsbad, CA), bovine serum albumin, selenium, putrescine, triiodo-thyronine, transferrin, progesterone, pyruvate (1 mM, Sigma; St. Louis, MO), glutamine (2 mM, Sigma; St. Louis, MO), ciliary neurotrophic factor (CNTF; 10 ng/mL; Regeneron Pharmaceuticals Inc.; Tarrytown, NY), brain-derived neurotrophic factor (BDNF; 50 ng/mL, Regeneron Pharmaceuticals Inc.; Tarrytown, NY), insulin (5 μg/mL; Sigma), and forskolin (10 μM, Sigma), as defined in Ullian et al. (2001). Cultures were maintained at 37° C in a humidified environment of 10% CO_2 / 90% O_2 (Praxair; Danbury, CT). Under these conditions, more than half of the RGCs survive *in vitro* for at least one month (Meyer-Franke et al., 1995).

Cortical astrocyte cultures were prepared from 1^{st}-2^{nd} day postnatal (P1-2) Sprague Dawley (SD) rats as previously described (McCarthy and de Vellis, 1980). Briefly, the cortex was dissected and digested in trypsin. Cells were plated in tissue culture flasks (BD Biosciences; San Jose, CA) in a medium that does not allow survival of neurons (Dulbecco's minimum essential medium, fetal bovine serum (10%), penicillin (100 U/mL), streptomycin (100 mg/mL), glutamine (2 mM) and Na-pyruvate (1 mM)). After 4 days in culture, nonadherent cells were removed from flasks by shaking. Remaining cells were removed from flasks enzymatically and cultured on poly-D-lysine (PDL; 70kDa, 10μg/mL; Sigma; St. Louis, MO) coated tissue culture plates (BD Biosciences; San Jose, CA) in astrocyte growth medium (Ullian et al., 2001). Astrocyte cultures could be maintained for long-term culture by routinely passaging confluent cultures by enzymatically removing astrocytes from culture plates and replating them at lower density on new plates.

Optic nerve astrocytes were prepared as previously described (Mi et al., 1999). Briefly, optic nerves were dissected from P5 rats and dissociated in trypsin. The optic nerve astrocytes were specifically purified using a sequential immunopanning procedure for negative selection and Ran-2 for positive selection. Astrocytes were then trypsinized off of the final panning plate and plated onto PDL coated coverslips.

Astrocytes were fixed with the addition of 100% methanol for 30 minutes at room temperature. Prior to plating RGCs in contact with fixed astrocytes, the fixed layers were rinsed three times with Dulbecco's Phosphate Buffered Saline at 2 hour intervals.

Labeling Purified Neurons

To specifically label either P5 or E17 neurons for heterochronic co-culture experiments, neurons were incubated at 37°C in CT-Cell tracer dye (Molecular Probes; Eugene, OR) for 15 minutes in EBSS. Dye containing EBSS was removed and replaced with full RGC growth

media for an additional 30 minutes. Cells were then rinsed 8 times with DPBS and trypsinized off the final panning plate.

Synaptic Assay and Immunocytochemistry

Following treatment, cultures were fixed for seven minutes at room temperature in 4% paraformaldehyde (PFA) pre-warmed to 37°C. The PFA was then aspirated off and cultures were washed three times with phosphate buffered saline (PBS). The coverslips were removed from the culture plate and 100μL of blocking buffer (50% Antibody buffer (0.5% bovine serum albumin, 0.5 % Triton X-100, 30 mM $NaPO_4$ (pH 7.4), 750 mM NaCl, 5% normal goat serum, and 0.4% NaN_3); 50% goat serum (NGS); 0.1% TritonX-100) was added for 30 minutes. After blocking, coverslips were washed three times in PBS. For staining of excitatory synapses, primary antibody solution contained monoclonal Rabbit anti-Rat Synaptotagmin (cytosolic domain, Synaptic Systems; Göttingen, Germany) and monoclonal Mouse anti-PSD-95 (6G6-1C9 clone, Affinity BioReagents; Golden, CO) diluted 1:500. 100μL of primary antibody solution was added to each coverslip. Coverslips were incubated overnight at 4°C. Following incubation, coverslips were washed five times in PBS. Secondary antibody solution containing Alexa-594 conjugated Goat anti-Rabbit and Alexa-488 conjugated Goat anti-Mouse (Molecular Probes; Eugene, OR) at a dilution of 1:500 in antibody buffer was added. Coverslips were incubated in secondary antibody solution for two hours at room temperature. Following incubation, coverslips were washed five times in PBS, then mounted in Vectashield mounting medium containing DAPI (a cellular nuclear marker) (Vector Laboratories Inc.; Burlingame, CA) on glass slides (VWR Scientific; West Chester, PA). Mounted coverslips were stored at -30°C until used. Mounted coverslips were imaged using Nikon Diaphot and Eclipse epifluorescence microscopes. Healthy cells that were at least 2 cell diameters from their nearest neighbor were identified and selected at random by eye using DAPI fluorescence. 8-bit digital images of the fluorescence emission at both 594nm and 488nm were obtained for each selected cell using a cooled monochrome CoolSnap camera and SPOT or Image Q, image capture software (Diagnostic Instruments, Inc.; St. Sterling Heights, MI). Each single-channel image was adjusted to remove unused portions of the pixel value range and the used pixel values were adjusted appropriately to utilize the entire pixel value range. Corresponding channel images were then merged to create a color (RGB) image containing the two single-channel images as individual color channels, using a custom software package called SpotRemover (©2001 Barry Wark. Source code or binaries available upon request to barrywark@mac.com). On Macintosh OS X, these manipulations can be performed automatically.

Synapses were identified by colocalization (overlap) of synaptotagmin and PSD-95 puncta. Although pre and postsynaptic sites do not actually overlap, the resolving power of light microscopy prevents distinguishing individual puncta at a single synapse. Colocalized puncta were identified and characterized using a custom written plug-in (©2001 Barry Wark. Source or binaries available upon request to barrywark@mac.com) for the NIH image processing package, ImageJ v1.24 and greater (available at http://rsb.info.nih.gov/ij/). Full documentation of the puncta counting algorithm is available in the “Puncta Analysis” plug-in’s source code. Briefly, the rolling ball background subtraction algorithm was used to remove low-frequency background from each image channel. The user was then prompted to “mask” the puncta in the single-channel image by thresholding the image so that only puncta remained above threshold. ImageJ’s “Particle Analyzer” plug-in was then used to identify and characterize puncta within each channel. Puncta in different color channels were defined as colocalized if the centers of two circles, centered at the puncta’s centroids and with areas equal to the puncta’s area, were less than the larger of the two circle’s radius apart. Number, mean area, mean minimum and maximum pixel intensities, and mean mean pixel intensities for all synaptotagmin, PSD-95, and colocalized puncta in the image were recorded and saved to disk for later analysis. Data analysis, including ANOVA was performed in SigmaStat (SPSS;

Chicago, IL). Unless noted, ANOVA was performed using the Student-Newman-Keuls method and ANOVA on ranks was performed using the Kruskal-Wallis method with Dunn's method of multiple comparison. Data visualization was completed in SigmaPlot (SPSS; Chicago, IL). All experiments were repeated 3 times with separate biological samples.

To characterize dendritic complexity cultured E17 and P5 neurons (prepared for staining as detailed above) were immunostained with monoclonal Mouse anti-MAP-2 (Chemicon; Temecula, CA), a dendrite specific marker. Images were visualized using Nikon 80i epifluorescence and captured with a cooled monochrome CoolSnap camera. Images were further analyzed by custom plug-ins for the NIH image processing package, ImageJ (available at http://rsb.info.nih.gov/ij/). To analyze individual dendritic fields single neurons were traced using NeuronJ (Meijering et al., 2004) (available at http://www.imagescience.org/meijering/software/neuronj/). Traced neurons were saved as 8-bit grayscale images and analyzed by a custom Sholl Analysis plug-in (available at http://www-biology.ucsd.edu/labs/ghosh/software/index.html). Radii for Sholl analysis were programmed to extend four cell body lengths from the soma, encompassing the same dendritic area used to quantify synapses (see above).

Immunohistochemistry

Whole heads from embryonic day 17 and 19 SD rats were fixed in 4% paraformaldehyde (in PBS) for 4 or 24 hours (E17 and E19 respectively). Heads were cryoprotected in 30% sucrose in PBS. Following cryoprotection tissues were sectioned by freezing microtome into 0.75μm sections in 0.1M Phosphate Buffer. Sections were washed three times with PBS followed by 30 minute room temperature (RT) blocking in 5% Normal Goat Serum, 0.25% Triton X-100 in PBS (Blocking Buffer). Blocking was followed by a 1 hour RT primary incubation using primary antibodies monoclonal Mouse anti-GFAP (Chemicon; Temecula, CA) 1:500 to visualize astrocytes and monoclonal Rabbit anti-Neuronal Class III β-tubulin (Covance; Berkeley, CA) 1:500 in PBS as a neuronal marker. Following primary incubation, sections were washed once with PBS. Secondary incubation with Alexa-594 conjugated Goat anti-Mouse and Alexa-488 conjugated Goat anti-Rabbit (Molecular Probes; Eugene, OR) was performed at a 1:500 dilution in Blocking Buffer for 1 hr at RT. Following secondary incubation sections were washed three times with PBS at RT and mounted using Vectashield with DAPI (Vector Laboratories Inc.; Burlingame, CA) onto glass slides (VWR Scientific; West Chester, PA).

Whole eyes were rapidly excised and fixed in 4% paraformaldehyde in Phosphate Buffer for 15-30 minutes. Tissue was cryoprotected overnight at 4°C (30% sucrose in PBS). 30 micron sections were mounted directly onto Fisherbrand Superfrost microscope slides (Fisher Scientific; Houston, TX). Blocking for 30 minutes at RT with Blocking Buffer was followed by an overnight primary incubation at 4°C in PBS, using monoclonal Rabbit anti-Neuronal Class III β-tubulin (Covance; Berkeley, CA) at a 1:1500 dilution to visualize neurons and monoclonal Mouse anti-Synaptic Vesicle Protein (SV)2 (Developmental Hybridoma Bank, University of Iowa) at a 1:100 dilution, as a presynaptic marker. Slides were washed in PBS and incubated for 3 hours at RT with secondary antibodies Alexa-594 conjugated Goat anti-Rabbit and Alexa-488 conjugated Goat anti-Mouse (Molecular Probes; Eugene, OR) diluted 1:1000 in Blocking buffer. Following secondary incubation, slides were washed three times with PBS and mounted using Vectashield with DAPI (Vector Laboratories Inc.; Burlingame, CA) onto glass slides (VWR Scientific; West Chester, PA). Staining was visualized with a Nikon Eclipse 80i epifluorescence microscope.

Neurexin and Neuroligin Staining

E17 RGCs cultured with and without astrocyte contact for 7-10 days *in vitro* (DIV) were stained for Chicken anti-pan-neurexin (kind gift of P. Scheiffele, 1:200) or Rabbit anti-pan-neurexin (Synaptic Systems; Göttingen, Germany, 1:500) and polyclonal Rabbit anti-pan-neuroligin (kind gift of P. Scheiffele, 1:400). Coverslips stained for neuroligin were fixed with a combined PFA/Methanol method. Briefly, cells were fixed with 4% paraformaldehyde solution for 10′ at RT, followed by a 2′ methanol permeablization at RT. Coverslips were washed five times with PBS followed by a primary antibody incubation overnight at 4°C. Neuroligin secondary staining and neurexin staining were performed as detailed above (see *Synaptic Assay and Immunocytochemistry*). Intensity of neurexin staining was quantified using the NIH image processing package, Image J. Equal exposure images acquired using Simple PCI software (Compix Inc.; Sewickley, PA), were converted to 8-bit grayscale images and background subtracted. Mean grayscale intensity measurements were made along a two pixel-width line along 12.5 μm lengths of dendrite using the measurement tool option. This allowed for the measurement of intensity along the dendrite only.

Transient Transfection

Embryonic RGCs were transiently transfected using the Effectene Cell Transfection Reagent (Qiagen; Valencia, CA) following manufacturer's instructions. Hemagglutinin (HA)-tagged neurexin (NRX) constructs were generously provided by Dr. Peter Scheiffele (NRX1β4(1)-HA, as described in Taniguchi et al., 2007). Following ten days in culture embryonic RGCs were fixed and processed for immunostaining as described above (See *Synaptic Assay* and *Immunostaining*). Synaptic markers, synaptotagmin and PSD-95 were used as pre and postsynaptic markers respectively (details provided above) and transfected neurons were visualized by immunostaining for the HA-tag using Chicken anti-HA (Chemicon; Temecula, CA) at a 1:250 dilution. Staining was visualized with a Nikon Eclipse 80i epifluorescence microscope.

Electrophysiology

Membrane currents were recorded using whole-cell patch-clamp techniques at a holding voltage of -70mV as previously described (Ullian et al., 2001). Patch pipettes (3-10 MΩ) were pulled from borosilicate glass (WPI; Sarasota, FL). External solution contained (in mM) 120 NaCl, 3 $CaCl_2$, 2 $MgCl_2$, 5 KCl, and 10 HEPES (pH 7.3). Internal pipette solution contained (in mM) 100 K-gluconate, 10 KCl, 10 EGTA (Ca^{2+}-buffered to 10^{-6}), and 10 HEPES (pH 7.3). All experiments were performed at room temperature (18-22°C). Whole-cell currents were recorded using pClamp software for Windows (Axon Instruments; Union City, CA). Mini excitatory post-synaptic events (mEPSCs) were recorded in the presence and absence of TTX (Alamone labs; Jerusalem, Israel), analyzed using Mini Analysis Program (SynaptoSoft; Decatur, GA) and plotted using SigmaPlot or Origin (Microcal; Northampton, MA).

Results

Purification of embryonic RGCs by immunopanning

To determine if embryonic neurons are capable of making synapses *in vitro*, we purified embryonic retinal ganglion cells from a variety of ages using an immunopanning procedure we previously developed for purification of postnatal RGCs (Barres et al., 1988). The purity of the postnatal RGCs isolated using this method is greater than 99.5%, as determined by retrograde labeling. As retrograde labeling of embryonic RGCs can not be used to confirm purity, we instead labeled immunopanned embryonic RGCs with early RGC specific markers; β-tubulin and Brn3b (Watanabe et al., 1991; Liu et al., 2000). E17 retinal sections stained with an anti-β-tubulin antibody, showed labeling of most cells in the ganglion cell layer (Sup. Fig.

1A), indicating its specificity at this age. We found that 100% of the neurons purified from E17 retina label with the anti-β-tubulin antibody indicating that they are highly purified RGCs (Sup. Fig 1B). Brn3b is a transcription factor expressed by most, but not all, RGCs as soon as they have differentiated (Liu et al., 2000). We found that anti-Brn3b specific antibody labels cells predominantly in the RGC layer of the embryonic retina (Sup. Fig.1C). Consistent with this conclusion, we detected Brn3b nuclear immunoreactivity in approximately 90% of the cells in our E17 RGC cultures (Sup. Fig. 1D), a percentage that is consistent with the percentage of RGCs in E17 retinal sections and purified postnatal RGCs that label with this antibody. In combination these two antigenic markers were used to assess the purity of the putative purified population of RGCs we isolated from E17 retina by immunopanning (see Experimental Procedures). In contrast, none of the purified neurons stained with the amacrine-specific marker VC1.1 (data not shown), the other main type of neuron present in E17 retinas. Taken together, these results indicate that the cells that we isolated from E17 retina are highly purified RGCs.

Embryonic RGCs have many fewer synapses than postnatal RGCs

Purified postnatal (P)5 RGCs are able to make numerous synaptic connections in response to soluble astrocyte signals. This effect has been characterized through the use of astrocyte feeding layers in which astrocytes are cultured on a porous membrane and placed over cultured neurons allowing for the diffusion of soluble astrocyte signals in the absence of direct neuron-glia contact (Mauch et al., 2001; Nagler et al., 2001; Ullian et al., 2001; Christopherson et al., 2005; Sup. Fig. 3). To determine if E17 neurons are able to form functional synapses under these conditions, we recorded spontaneous synaptic activity from cultured E17 or P5 neurons (Fig. 1C). We found that, as expected, P5 neurons had high rates of spontaneous synaptic activity, displaying on average 100 ± 24 synaptic events/minute, mean ± SEM. In contrast, E17 neurons displayed very low rates of spontaneous synaptic activity, about 50 times less activity than the P5 neurons (2 ± 1 events/minute, mean ± SEM, $p < 0.05$, t-test).

The lower level of spontaneous synaptic activity exhibited by E17 neurons might result from nonfunctional or decreased numbers of synapses. To quantify synapse number we immunostained purified RGCs cultured with astrocyte feeding layers for presynaptic synaptotagmin and postsynaptic PSD-95. We previously found that these two synaptic markers colocalize when mature structural synapses are present between RGCs (Ullian et al., 2001). As expected, immunostaining of P5 neurons cultured with astrocyte feeding layers, revealed numerous synaptic puncta along dendrites and in somas with clear co-localization of pre and postsynaptic markers (Fig. 1B). In contrast, E17 neurons exhibited few such synaptic puncta under the same culture conditions (i.e. with astrocyte feeding layers) and even after 4 weeks in culture (Fig. 1A). Quantification of the number of colocalized synaptic puncta indicates that there is a nearly 10-fold increase in the number of synapses formed on pure P5 neurons compared to pure E17 neurons ($p < 0.05$, t-test).

E17 RGCs can form but not receive synapses

Do E17 RGCs exhibit few synapses because they cannot form synapses onto each other, because they cannot receive synapses from each other, or both? To distinguish between these possibilities, we co-cultured neurons of different ages (here E17 and P5), repeating the "heterochronic" culture experiments of Fletcher et al. (1994). By culturing high density E17 RGCs with low density, dye-labeled P5 RGCs for one week (Fig. 2A) we were able to assess the ability of E17 RGCs to form synapses. Under these conditions the majority of synaptic inputs onto P5 RGCs will be from the much higher density E17 RGCs, allowing us to determine if the E17 RGCs are capable of forming normal synapses. We found that the high density E17 neurons formed numerous structural and functional synapses onto P5 neurons. Immunostaining co-cultures of high density E17 neurons and low density P5 neurons revealed numerous synaptic puncta along the dendrites of the P5 neurons (Fig. 2B-E). The total number of synapses

formed on P5 neurons, about 40 synapses per neuron, is similar to the total number found in pure cultures of P5 neurons, about 30 synapses per neuron (Fig. 2G, left), indicating that E17 neurons are as good as P5 neurons at forming synapses. These synapses were fully functional as assessed by the frequency and amplitude of spontaneous synaptic events (Fig. 2F, top, G, right). These data show that E17 RGCs are capable of forming synapses when allowed to contact more mature receptive neurons. Interestingly, we saw few synapses formed on E17 neurons under these conditions.

To investigate the synaptic receptivity of E17 RGCs, we performed another heterochronic experiment, this time co-culturing low density dye-labeled E17 RGCs with high density P5 RGCs. Under these conditions the majority of synaptic inputs onto the E17 RGCs will be from the P5 RGCs. These conditions allow us to assess the ability of the E17 RGCs to receive synapses from postnatal RGCs and serve as a measure of synaptic receptivity because postnatal RGCs are competent to form synapses in response to astrocyte feeding layers. Under these conditions few structural synapses were formed by the P5 neurons onto the E17 neurons, as judged by immunostaining (data not shown). Similarly, few functional synapses onto the embryonic neurons could be detected by whole-cell patch-clamp recordings (Fig. 2F, bottom, G, right.; 7 ± 3 events/minute, mean ± SEM). Thus both E17 and P5 RGCs were able to robustly form functional synapses, but E17 RGCs, unlike their postnatal counterparts, exhibited little ability to receive synapses.

Synaptic Receptivity of E17 RGCs is not determined by dendritic elaboration

We next investigated whether the inability of E17 RGCs to receive synapses was due to insufficient dendrite elaboration. Previous reports indicate that embryonic RGCs extend axons robustly but are relatively poor at growing dendrites, until induced to do so by amacrine contact at P0 (Goldberg et al., 2002). It is possible that E17 neurons receive few synapses simply because they do not extend numerous dendritic arbors and thus have less area to receive synapses (Fletcher et al., 1994; Withers et al., 2000). Interestingly, we found that we could induce substantial dendritic growth in E17 RGCs when cultured under astrocyte-feeding layers for a prolonged culture period of 2 weeks, the same conditions used to quantify synapse formation. We labeled co-cultured E17 and P5 neurons grown 2 weeks in culture with antibodies against the dendritic marker MAP-2 (Fig. 3A-C). Detailed analysis revealed no statistically significant change in the number of primary dendrites on E17 and P5 neurons after two weeks in culture (Fig 3G, $p > 0.05$, t-test). We further analyzed dendritic complexity by Sholl analysis and found no statistically significant difference in dendritic complexity between E17 and P5 neurons (Fig. 3D-F, $p > 0.05$, t-test).

To confirm that these E17 RGCs with long dendrites were not capable of receiving synapses, we immunostained the co-cultured labeled P5 RGCs with unlabeled E17 RGCs for MAP-2 and synaptic markers and confirmed that the E17 RGCs were unable to receive many synaptic inputs along robust MAP-2 positive dendrites (Fig. 4A-F). Therefore, the inability of E17 neurons to receive synapses cannot be explained by a lack of dendrites. Moreover these data demonstrate that E17 RGCs do not acquire synaptic receptivity as a result of an intrinsic maturation program because a prolonged 2 week culture period (one that mimics the age when all of the cells would have been synaptically receptive had they been left *in vivo*) does not result in synaptic receptivity.

Onset of synaptic receptivity requires contact with retinal cell types

RGCs begin to contact other cell types during the later stages of embryonic development. Although E17 neurons do not form many synapses as previously described, by E19, RGCs are capable of forming numerous synapses *in vitro* (E19: 27.5 ± 3.2; P5: 30.7 ± 4.7 colocalized synaptic puncta/cell, $p < 0.05$, Kuskal Wallis AVOVA). These data indicate that although

RGCs exhibit little synaptic receptivity at E17, they have rapidly acquired it by E19. Because E17 RGCs do not acquire synaptic receptivity over time in culture and E19 RGCs maintain synaptic receptivity acquired *in vivo* for prolonged culture periods *in vitro* (i.e. 4 weeks, data not shown), this strongly suggests that the retinal and/or optic environment is responsible for inducing synaptic receptivity at E19. To test this hypothesis, we co-cultured labeled E17 neurons with mixed retinal cells (isolated by dissociation of whole retina) for 14 days to assess synaptic receptivity. We found that the E17 neurons cultured with mixed retinal cells were able to receive numerous synaptic inputs as assessed by patch-clamp recording of spontaneous synaptic currents (Fig. 5A, B) and by immunostaining (Fig 5D, F). This switch did not occur when the RGCs were placed below a feeding layer of mixed retinal cells (MRFL), but only when they were in direct contact with them (Fig. 5A, B). These results indicate that the retina provides a contact-mediated signal that induces synaptic receptivity in embryonic RGCs.

Astrocyte contact, but not amacrine contact induces synaptic receptivity in RGCs

In retina, there are three cell types in the vicinity of the RGCs at the onset of synaptic receptivity (E19): cones, amacrine cells, and astrocytes (both in the retinal optic nerve fiber layer and optic nerve). Of these three, we can highly purify and culture amacrines and astrocytes. Because amacrine cells provide a major synaptic input onto RGCs, we first tested whether their presence would be sufficient to induce synaptic receptivity. We co-cultured E17 RGCs in contact with purified amacrine cells and then determined the number of structural and functional synapses after 14 days of co-culture. When we recorded from E17 RGCs cultured with amacrine cells, we did not find an increase in spontaneous excitatory synaptic events with patch-clamp recordings, even when cultured with a feeding layer of astrocytes (Fig. 5A, B). We also did not find an increase in the number of structural synapses when we immunostained these cultured for synaptic markers (Fig. 5C, E). These results indicate that amacrine cells, despite their strong dendrite inducing ability (Goldberg et al., 2002), do not provide the signal for receptivity in E17 neurons.

Astrocyte precursor cells invade the retina from the optic nerve beginning around E17, and numerous astrocytes have migrated into the ganglion cell layer of the retina by E19 (Huxlin et al, 1992.; Johnson et al., 1997). Furthermore, astrocyte precursor cells within the optic nerve do not differentiate into astrocytes until E19 (Mi et al., 1999), nearly the same time as the observed *in vitro* switch in synaptic receptivity. To determine if astrocytes can provide a contact-mediated induction of synaptic receptivity in E17 RGCs, we co-cultured E17 RGCs with purified optic nerve astrocytes for 14 days (Sup. Fig. 3). We found that under these culture conditions, E17 RGCs received numerous synapses as measured by immunostaining for synaptic markers (Fig. 5G, I). Quantification of synaptic puncta on E17 RGCs grown in contact with astrocytes indicate that astrocyte contact increases synapse number 10-fold (1.8 ± 0.5 no astrocyte contact vs. 17.9 ± 1.4 astrocyte contact; $p = 0.009$). When compared to conditions of direct contact with amacrine cells synaptic puncta on E17 RGCs increased nearly 9-fold when cultured in direct contact with mixed retinal cells (1.36 ± 0.41; 11.7 ± 2.23; $p = 0.005$) and 19-fold when cultured in direct contact with astrocytes (1.36 ± 0.41; 26.5 ± 2.49; $p = 0.00012$) (Fig. 5H). Patch-clamp recordings revealed a large increase in spontaneous synaptic currents, indicating that the synapses formed in culture are fully functional (average peak amplitude was -56.7 +/- 6.3 pA, and the average frequency was 3.5 +/- 0.7 Hz) (Fig. 5J). These results indicate that astrocytes provide a contact-mediated signal allowing E17 neurons to receive synapses. We next asked if the contact mediated effect requires signaling from live cells or is preserved in fixed astrocyte membranes. We fixed live beds of astrocytes with methanol (100%), washed the fixed cells with DPBS and plated labeled E17 RGCs on the astrocyte membranes and cultured them for 14 days. Under these conditions we saw a slight 4-fold increase in synapse number (1.75 ± 0.5 no contact vs. 9.2 ± 0.9 fixed astrocyte contact; $p = 0.009$), indicating that a portion of activity is preserved in fixed membranes. We next wondered whether contact with

astrocyte membranes could induce a switch in the ability of E17 neurons to respond to Thrombospondin (TSP). TSP is an extracellular matrix protein previously shown to be a soluble astrocyte-secreted factor competent to induce structural synapse formation (Christopherson et. al, 2005). We fixed both astrocytes and amacrines from postnatal day 5 SD rats and plated E17 RGCs on each. Even with the repeated addition of TSP over a two week culture period synapse formation was not significantly different between E17 neurons cultured on fixed astrocytes with and without TSP treatment (data not shown, 14% increase in synapses over control; $p = 0.21$), indicating that induction of synaptic receptivity by astrocyte contact is mechanistically distinct from the increase in synapse number caused by TSP.

In addition, astrocyte contact did not induce significant changes in E17 dendritic morphology as assessed by Sholl analysis (Fig. 3) indicating that astrocyte contact increases synaptogenesis independently of dendrite outgrowth.

Astrocyte contact has been found to increase synapse number on embryonic hippocampal neurons in a PKC-dependent manner (Hama et al., 2004). Is this mechanism conserved in retinal ganglion cells? We tested the necessity and sufficiency of PKC signaling in increasing synapse number in embryonic RGCs. E17 neurons treated with activators of the PKC signaling pathway did not show an increase in synaptic puncta (data not shown) and blocking PKC signaling did not significantly interfere with the ability of astrocyte contact to increase synapse number on E17 neurons (17.9 ± 1.4 astrocyte contact vs. 23.7 ± 2.5 astrocyte contact + GFX (an inhibitor of PKC action); $p > 0.05$). Thus, unlike for hippocampal neurons, the PKC signaling pathway does not appear to be sufficient or necessary for astrocyte contact-mediated increases in synapse number in developing RGCs.

The astrocyte contact dependent induction of synaptic receptivity also does not depend on synaptic activity. We cultured E17 RGCs on astrocytes in the presence and absence of TTX and CNQX to block all synaptic transmission (all spontaneous synaptic transmission is mediated by AMPARs (Ullian et al., 2004b)). Under these conditions we found no difference in the number of synaptic puncta or in the frequency of spontaneous mEPSCs between the treated and untreated control cultures indicating that synapse formation is not activity dependent.

We next asked, what is the exact relationship between the appearance of astrocytes in the retina and synaptogenesis? We immunostained E16, E19, E21, and P4 retinas for neuronal and astrocyte markers. Previous studies have reported astrocytes migrating into the retina around E18-E19 (Huxlin et al, 1992; Johnson et al., 1997; Mi et al., 1999). Similarly, we found evidence for GFAP-positive astrocytes in E19 retina (Sup. Fig. 2A-F). We next investigated the appearance of synaptic markers in the retina. Ultrastructural synapses, with clear vesicle accumulation and synaptic densities, first appear around P3 (Olney, 1968), but prior to this numerous contacts are made in the retina as synapses begin to form. To visualize the development of these contacts, we labeled RGCs and their dendrites with β-tubulin and innervating axons with Synaptic Vesicle Protein 2 (SV2). We found at E16-17 there were very few SV2 puncta associated with RGCs indicating that very few synaptic contacts have begun to form (Sup. Fig. 2G-J). By E19 however, we found a dramatic increase in the accumulation of SV2 immunoreactivity from the synaptic layer onto RGCs (Sup. Fig. 2K-N). The accumulating SV2 is both increasingly punctate and intense, with distinct puncta visible from E21 (Sup. Fig. 2O-R) to P4 (Sup. Fig. 2S-V) in line with the time course of ultrastructural synapse formation in the retina. Thus, the acquisition of synaptic receptivity by E19 RGCs temporally matches both the appearance of astrocytes and the formation of synapses *in vivo*.

Finally, we asked what potential mechanisms could contribute to the regulation of synaptic receptivity in embryonic neurons. To answer this question we used immunostaining to screen

embryonic neurons cultured with and without astrocyte contact for adhesion molecules involved in synaptogenesis. We analyzed the localization of numerous proteins including N-cadherin, β-catenin, neuroligin, and neurexin. Most of these markers were localized in dendrites and changed from a diffuse to a punctuate pattern of staining consistent with their reported changes upon synapse formation (Benson et al. 1998, Song et al. 1999, Taniguchi et al. 2007). Neurexin, however, dramatically changed from high dendritic localization to low dendritic localization in E17 neurons upon contact with astrocytes (Fig. 6A,C). E17 neurons cultured in the absence of astrocyte contact displayed robust neurexin staining in dendrites (Fig. 6A, D). In contrast, E17 neurons cultured in contact with astrocytes showed a three-fold reduction in neurexin immunoreactivity in dendritic compartments (Fig. 6C, F, H). Interestingly, the reduction in neurexin dendritic localization does not occur in response to the soluble astrocyte signal, TSP (Fig. 6B, E, H). This result suggests that astrocyte contact provides signals that both reduce dendritic neurexin and confer synaptic receptivity. We next wondered whether dendritic expression of neurexin in embryonic neurons might account for their reduced synaptogenic ability compared to P5 neurons. In P5 RGCs neurexin immunoreactivity is reduced in dendrites when compared to E17 (Fig. 6G; 48.2 +/- 4.8 mean grayscale value/ 12.5 μm length of dendrite P5 vs. 64.9 +/- 4.1 E17 mean grayscale value/12.5 μm length of dendrite; $p = 0.027$). Neuroligin however, remained in dendritic compartments under all conditions and changed from a diffuse localization in E17 neurons without astrocyte contact to a highly punctate localization in E17 neurons with astrocyte contact, consistent with the reported changes associated with synapse formation (Fig. 6I-L).

We were able to assess changes in the expression level of some neurexin (NRX) and neuroligin (NLG) isoforms through the use of RT-PCR and Western Blotting. When comparing retinal lysates from E17 and P5 we find a less than 3% reduction in protein levels of neurexin β-isoforms (Sup. Fig. 4C). During this same timeframe (E17 to P5) we note a large reduction in NRX1β mRNA (Sup. Fig. 4A, 84%) and an increase in NRX2β mRNA (Sup. Fig. 4A, 70%). mRNA levels of NLG1 appear to increase slightly during this timeframe (Sup. Fig. 4B; 23%). Interestingly, postsynaptic neurexin expression has been reported to reduce synapses (Taniguchi et al., 2007) raising the possibility that postsynaptic neurexin expression is a mechanism used by developing neurons to regulate the timing of synapse formation. If astrocyte contact mediates synaptic receptivity in part by redistributing neurexin, we predict persistent dendritic expression of neurexin will attenuate synaptic receptivity resulting from contact between astrocytes and developing neurons. Indeed we find that dendritic expression of an hemagglutinin (HA)- tagged neurexin1 β isoform in E17 RGCs cultured on astrocytes blocks the induction of synaptic receptivity in these neurons. (Fig. 7 A-F). This effect was highly significant ($p = 0.00004$).

Discussion

Newly-generated RGCs can form synapses upon more mature neurons but are not competent to receive them

Although it was generally thought that neurons in the developing brain were generated with the ability to both form and receive synapses, elegant studies by Banker and colleagues had shown that axons and dendrites of embryonic hippocampal neurons in culture became competent for synaptogenesis at different stages of development (Fletcher et al., 1994). In these studies, hippocampal neurons developed a significant number of synapses, as measured by immunostaining, concurrent with their elaboration of dendrites or in response to BMP-7 stimulation (Fletcher et al., 1994; Withers et al., 2000). These studies suggested that a dendrite maturation dependent program controlled the acquisition of synaptic receptivity by controlling the timing of dendritic arborization.

Our findings add to the understanding of how newly formed neurons in the developing CNS acquire competence to receive synapses by demonstrating that two distinct mechanisms are present, one determining dendrite elaboration and a second controlling synaptic receptivity. By studying the ability of highly purified RGCs in culture to both form and receive synapses, we found that RGCs from the earliest stage that we could purify them, E17, were capable of forming synapses upon more mature neurons (here P5 neurons), and were induced by other cell types to become competent to receive synapses at E19. RGCs under the age of E19 were unable to receive synapses even when cultured for several weeks suggesting that receptivity is not due to a purely intrinsic mechanism. Thus, synaptic receptivity appears during a short window of development, between embryonic days 17 and 19. We were able to clearly distinguish the acquisition of synaptic receptivity from the generation and elaboration of dendrites. Remarkably, E17 RGCs after 2 weeks in culture with astrocyte feeding layers elaborate long dendrites, yet continue to be synaptically unreceptive. Because their axons are able to form synapses without difficulty, these findings point to the existence of an as yet unidentified postsynaptic mechanism in E17 RGCs that controls their synaptic receptivity. This mechanism might be accounted for either by the presence of a molecule that inhibits synaptogenesis or the absence of a molecule necessary for synaptogenesis (with synaptogenesis defined as any mechanism that increases synapse number by enhancing the rate of synapse formation or synaptic stability). Our evidence provides support for the former.

Competence to receive synapses is induced by extrinsic signals from neighboring retinal or optic nerve cells, and by direct contact with retinal astrocytes

How is competence to receive synapses acquired by RGCs at E19? Our findings show that it does not occur as the result of an age-dependent intrinsic mechanism and that dendrite formation and elaboration are also insufficient. Rather, we found that contact-mediated signals from other retinal and optic nerve cell types are sufficient to induce synaptic receptivity. This change is reminiscent of, but mechanistically distinct from, a similar change we have previously identified at P0 in RGCs. We found that embryonic RGCs are capable of extending axons rapidly but dendrites slowly, whereas at P0 they lose the intrinsic ability to extend their axons rapidly but gain the ability to rapidly elaborate dendrites. This change is triggered by amacrine contact abruptly at P0 and is apparently irreversible (Goldberg et al., 2002). In contrast, here we have found that embryonic neurons are not competent to receive synapses but abruptly acquire this competence at E19, and that here amacrine cells are not able to induce this switch.

Our findings indicate that once an RGC has been generated from a progenitor cell it does not yet contain all the properties of a fully functional neuron, but must be signaled though a series of cell-cell interactions to become fully mature. In particular, they raise the question, how is the acquisition of competence for synaptic receptivity signaled? Possible cell types that could provide this signal *in vivo* include afferent inputs onto the neuron, target contact by RGC axons, or contact by glial cells within the retina, optic nerve fiber layer, or along the optic nerve. Our initial results showed that direct contact with mixed retinal cells was sufficient to induce synaptic receptivity, helping to focus our search. The two most relevant retinal neurons with potential synaptic inputs onto RGCs at E19 are amacrine cells and cone photoreceptors (Wong et al., 1992; Lohmann et al., 2002). Other retinal neurons that might synapse upon RGCs, such as bipolar neurons, are largely generated after E19. We were unable to purify the cone photoreceptors, but were able to directly test the possible effects of amacrine cells by purifying them and co-culturing them with E17 RGCs. We found they were insufficient to induce synaptic receptivity, despite their ability to greatly enhance dendritic elaboration.

Glial cells make extensive direct contact with RGCs at E19, both the Müller glia within the retina and astrocytes within the retinal optic nerve fiber layer and optic nerve. Few Müller glia

are generated by E19, however, astrocyte precursor cells are extensively differentiating into astrocytes in both the retina and optic nerve (Huxlin et al, 1992; Johnson et al., 1997; Mi et al., 1999) at E19, occurring almost exactly with the switch in synaptic receptivity. We found that co-culture of E17 RGCs in direct contact with optic nerve astrocytes was sufficient to induce the RGCs to acquire synaptic receptivity. These results implicate astrocyte contact as a likely inducer of synaptic receptivity, but it remains to be determined whether other retinal cell types might also contribute.

Support for the notion that astrocytes provide the *in vivo* signal for synaptic receptivity comes from observations of the timing of astrocyte ingrowth to the retina and the beginnings of synapse formation. We found that the first GFAP positive astrocytes appear at the time of the switch in synaptic receptivity (E19) and this corresponds to synaptic vesicle accumulation in the retinal synaptic layer of the RGCs, beginning at E19 and continuing until bona fide synapses are first detected at P3 (Sup. Fig. 2; Olney, 1968). Thus, the formation of synapses *in vivo* supports our findings of the development of synaptic receptivity *in vitro*, and strongly implicates astrocytes as one component of the developmental switch.

Recently, embryonic hippocampal neurons have also been found to be induced to form synapses by astrocyte contact. In this case astrocyte contact leads to an integrin-dependent activation of PKC that in turn leads to global synapse formation (Hama et al., 2004). It is not clear from these studies however, if this represents a switch in the ability of hippocampal neurons to make or receive synapses since the study used autaptic cultures. Our findings add to the understanding of synapse formation by showing 1) that newly generated neurons are not fully competent to receive synapse but must be signaled during development to do so and 2) dendrite outgrowth is mechanistically distinct from synaptic receptivity and 3) astrocytes provide a contact-mediated signal(s) that can at least in part induce the switch to receptivity.

Astrocytes promote synapse formation by at least two mechanisms

Taken together with previous studies (Pfrieger et al., 1997; Nagler et al., 2001; Mauch et al., 2001; Ullian et al., 2001; Song et al., 2002a, b) the present findings indicate that astrocytes induce synaptogenesis by at least two different mechanisms. First, they induce the acquisition of competence for synaptic receptivity. This effect requires direct contact of the astrocytes with RGCs. Second, astrocytes release soluble signals such as thrombospondin that greatly increase synapse number. This effect is highly reversible, as these astrocyte-derived soluble signals are necessary for synaptic maintenance (Ullian et al., 2001). The present findings add to the rapidly growing body of evidence that astrocytes are highly specialized to support, regulate, and control synaptic function and plasticity.

Despite these differences, are these two mechanisms by which astrocytes induce synapses nonetheless related? One simple possibility is that the receptors for the soluble synapse-inducing proteins secreted by astrocytes are induced in the RGCs, or directed to their dendrites, by direct astrocyte contact. Another possibility is that the receptors are constitutively present in the dendrites but are functionally inhibited or inaccessible prior to astrocyte contact. Astrocyte contact most likely induces synaptic receptivity by acting postsynaptically since the E17 RGCs are able to form synapses without difficulty onto the dendrites of more mature neurons. One possible mechanism by which astrocyte contact regulates the timing of synaptic receptivity is by altering the localization of neurexin. We have found that neurexin immunoreactivity is high on E17 dendrites without astrocyte contact and this immunoreactivity is dramatically reduced in E17 neurons in contact with astrocytes. Recently, it has been reported that neurexin is expressed at low levels at postsynaptic sites in more mature hippocampal neurons and that increasing postsynaptic expression of neurexin can reduce synapse number. Thus, the number or timing of synapse formation may be regulated by regulating the levels of postsynaptic neurexin expression (Taniguchi et al., 2007). Our findings extend this observation

by showing that neurons purified from early retina continue to exhibit high levels of diffuse dendritic neurexin, while neurons purified from postnatal retina have reduced localization of neurexin in their dendrites suggesting that mechanisms controlling the expression or localization of neurexin can change in neurons. Earlier studies have demonstrated the differential expression patterns of the three neurexin genes both in the adult and developing brain (Ushkaryov et al., 1992, Ullrich et al., 1995, Püschel et al., 1995). More recent studies show an upregulation of specific neurexin transcripts in response to insult (Górecki et al., 1999, Sun et al., 2000). It is of interest to note that mRNA levels of NRX1β are reduced from E17 to P5 in retina, while another neurexin gene β-isoform (NRX2β) shows increased levels of transcription during this time. While we can not definitely localize these changes to retinal ganglion cell dendrites further experiments may show neuronal compartment or developmental specificity for the neurexin family members perhaps as a means of fine-tuning the positioning and timing of synaptogenesis. Finally, we are able to block astrocyte induced synaptic receptivity in embryonic neurons by expressing high levels of neurexin dendritically. We find that dendritic overexpression of the β-isoform of a single neurexin gene (NRX1) is sufficient to attenuate astrocyte contact mediated effects on synaptic receptivity, extending our understanding of potential mechanisms by which astrocyte contact influences the developing dendrite. The present findings that astrocytes can induce synapse formation by inducing competence for synaptic receptivity independently of dendrite outgrowth expand our understanding of synaptic circuit formation and add to the rapidly growing body of evidence that astrocytes are highly specialized to support, regulate, and control synaptic function and plasticity.

Acknowledgments

This work was supported by the Zaffaroni Fellowship, Sandler Family Fund, Alfred P. Sloan Foundation, The March of Dimes Basil O'Connor Award, Research to Prevent Blindness Young Investigator Award, the Autism Speaks Foundation, That Man May See (E.M.U.), the National Institutes of Health (NIH)-National Eye Institute (NEI) Grant T32EY07120 (S.M.K.) and the National Institute of Drug Addiction (DA15043; B.A.B.). We thank Dr. Peter Scheiffele for anti-neurexin and neuroligin antibodies and neurexin-HA constructs.

References

Barres BA, Silverstein BE, Corey DP, Chun LL. Immunological, morphological, and electrophysiological variation among retinal ganglion cells purified by panning. Neuron 1988;1:791–803. [PubMed: 2908449]

Benson DL, Tanaka H. N-cadherin redistribution during synaptogenesis in hippocampal neurons. J. Neuroci 1998;18(17):6892–6904.

Bolliger MF, Pei J, Maxeiner S, Boucard AA, Grishin NV, Südhof TC. Unusually rapid evolution of Neuroligin-4 in mice. PNAS 2008;105:6421–6426. [PubMed: 18434543]

Bottenstein J, Hayashi I, Hutchings S, Masui H, Mather J, McClure DB, Ohasa S, Rizzino A, Sato G, Serrero G, Wolfe R, Wu R. The growth of cells in serum-free hormone-supplemented media. Methods Enzymol 1979;58:94–109. [PubMed: 423795]

Christopherson K, Ullian EM, Stokes CA, Mullowney CE, Hell JW, Agah A, Lawler J, Mosher D, Bornstein P, Barres BA. Thrombospondins are astrocyte-derived proteins that promote CNS synaptogenesis. Cell 2005;120:421–433. [PubMed: 15707899]

Craig AM, Kang Y. Neurexin-neuroligin signaling in synapse development. Curr. Opin. Neurobiol 2007;17:43–52. [PubMed: 17275284]

Dean C, Dresbach T. Neuroligins and neurexins: linking cell adhesion, synapse formation and cognitive function. Trends Neurosci 2006;1:21–9. [PubMed: 16337696]

Fletcher TL, De Camilli P, Banker G. Synaptogenesis in hippocampal cultures: evidence indicating that axons and dendrites become competent to form synapses at different stages of neuronal development. J Neurosci 1994;14:6695–6706. [PubMed: 7965070]

Goldberg JL, Klassen MP, Hua Y, Barres BA. Amacrine-signaled loss of intrinsic axon growth ability by retinal ganglion cells. Science 2002;296:1860–1864. [PubMed: 12052959]

Górecki DC, Szklarczyk A, Lukasiuk K, Kaczmarek L, Simons JP. Differential seizure-induced and developmental changes of neurexin expression. Mol Cell Neurosci 1999;13:218–227. [PubMed: 10408888]

Hama H, Chikako Hara, Kazuhiko Yamaguchi, Atsushi Miyawaki. PKC Signaling Mediates Global Enhancement of Excitatory Synaptogenesis in Neurons Triggered by Local Contact with Astrocytes. Neuron 2004;41:405–415. [PubMed: 14766179]2004

Huxlin KR, Sefton AJ, Furby JH. The origin and development of retinal astrocytes in the mouse. J Neurocytol 1992;21:530–544. [PubMed: 1500949]

Johnson PT, Geller SF, Lewis GP, Reese BE. Cellular retinaldehyde binding protein in developing retinal astrocytes. Exp Eye Res 1997;64:759–766. [PubMed: 9245906]

Liu W, Khare SL, Liang X, Peters MA, Liu X, Cepko CL, Xiang M. All Brn3 genes can promote retinal ganglion cell differentiation in the chick. Development 2000;127:3237–3247. [PubMed: 10887080]

Lohmann C, Myhr KL, Wong RO. Transmitter-evoked local calcium release stabilizes developing dendrites. Nature 2002;418:177–181. [PubMed: 12110889]

Mauch DH, Nagler K, Schumacher S, Goritz C, Muller EC, Otto A, Pfrieger FW. CNS synaptogenesis promoted by glia-derived cholesterol. Science 2001;294:1354–1357. [PubMed: 11701931]

McCarthy KD, de Vellis J. Preparation of separate astroglial and oligodendroglial cell cultures from rat cerebral tissue. J Cell Biol 1980;85:890–902. [PubMed: 6248568]

Meijering E, Jacob M, Sarria JCF, Steiner P, Hirling H, Unser M. Design and Validation of a Tool for Neurite Tracing and Analysis in Fluorescence Microscopy Images. Cytometry 2004;58A:167–176. [PubMed: 15057970]

Meyer-Franke A, Kaplan MR, Pfrieger FW, Barres BA. Characterization of the signaling interactions that promote the survival and growth of developing retinal ganglion cells in culture. Neuron 1995;15:805–819. [PubMed: 7576630]

Mi H, Barres BA. Purification and characterization of astrocyte precursor cells from the developing rat optic nerve. J. Neurosci 1999;19:1049–61. [PubMed: 9920668]

Nagler K, Mauch DH, Pfrieger FW. Glia-derived signals induce synapse formation in neurons of the rat central nervous system. J Physiol 2001;533:665–679. [PubMed: 11410625]

Olney JW. An electron microscopic study of synapse formation, receptor outer segment development, and other aspects of developing mouse retina. Invest Ophthalmol 1968;3:250–68. [PubMed: 5655873]

Pfrieger FW, Barres BA. Synaptic efficacy enhanced by glial cells in vitro. Science 1997;277(5332): 1684–7. [PubMed: 9287225]

Püschel AW, Betz H. Neurexins are differentially expressed in the embryonic nervous system of mice. J Neurosci 1995;15:2849–2856. [PubMed: 7722633]

Song JY, Ichtchenko K, Südhof TC, Brose N. Neuroligin 1 is a postsynaptic cell-adhesion molecule of excitatory synapses. Proc. Natl. Acad. Sci. USA 1999;96(3):1100–1105. [PubMed: 9927700]

Song H, Stevens CF, Gage FH. Astroglia induce neurogenesis from adult neural stem cells. Nature 2002a; 417:39–44. [PubMed: 11986659]

Song HJ, Stevens CF, Gage FH. Neural stem cells from adult hippocampus develop essential properties of functional CNS neurons. Nat Neurosci 2002b;5:438–445. [PubMed: 11953752]

Sun HB, Yokota H, Chi XX, Xu ZC. Differential expression of neurexin mRNA in CA1 and CA3 hippocampal neurons in response to ischemic insult. Brain Res Mol Brain Res 2000;84:146–149. [PubMed: 11113542]

Taniguchi H, Gollan L, Scholl FG, Mahadomrongkul V, Dobler E, Limthong N, Peck M, Aoki C, Scheiffele P. Silencing of neuroligin function by postsynaptic neurexins. J Neurosci 2007;27:2815–2824. [PubMed: 17360903]

Ullian EM, Sapperstein SK, Christopherson KS, Barres BA. Control of synapse number by glia. Science 2001;291:657–661. [PubMed: 11158678]

Ullian EM, Harris BT, Wu A, Chan JR, Barres BA. Schwann cells and astrocytes induce synapse formation by spinal motor neurons in culture. Mol Cell Neurosci 2004a;25:241–51. [PubMed: 15019941]

Ullian EM, Barkis WB, Chen S, Diamond JS, Barres BA. Invulnerability of retinal ganglion cells to NMDA excitotoxicity. Mol Cell Neurosci 2004b;26:544–57. [PubMed: 15276156]

Ullrich B, Ushkaryov YA, Südhof TC. Cartography of Neurexins: More than 1000 isoforms generated by alternative splicing and expressed in distinct subsets of neurons. Neuron 1995;14:497–507. [PubMed: 7695896]

Watanabe M, Rutishauser U, Silver J. Formation of the retinal ganglion cell and optic fiber layers. J Neurobiol 1991;22:85–96. [PubMed: 2010752]

Withers GS, Higgins D, Charette M, Banker G. Bone morphogenetic protein-7 enhances dendritic growth and receptivity to innervation in cultured hippocampal neurons. Eur. J. Neurosci 2000;12:106–16. [PubMed: 10651865]

Wong RO, Yamawaki RM, Shatz CJ. Synaptic Contacts and the Transient Dendritic Spines of Developing Retinal Ganglion Cells. Eur J Neurosci 1992;4:1387–1397. [PubMed: 12106402]

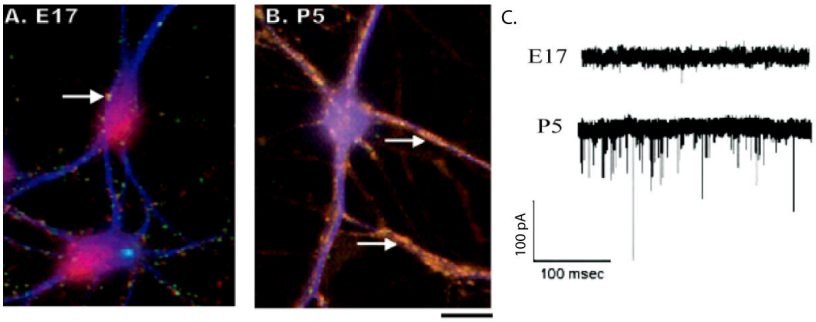

Figure 1.

Examples of RGCs purified from E17 and P5 retina and stained for synaptic markers synaptotagmin (red) and PSD-95 (green) after two weeks in culture. **A.** E17 RGCs with astrocyte feeding layers show few synaptic puncta and relatively little overlap of pre- (red) and post- (green) synaptic markers (arrow). **B.** In contrast to E17, P5 neurons with astrocyte feeding layers show numerous synaptic puncta as illustrated by overlap of red and green, pre and postsynaptic markers (yellow; arrows). Quantification of colocalized synaptic puncta on E17 and P5 neurons show nearly a ten-fold difference in the number synaptic puncta formed by P5 neurons ($p < 0.05$, t-test). **C**. Whole-cell voltage clamp recordings from E17 neurons show low levels of spontaneous synaptic activity (downward deflections). Whole-cell voltage clamp recordings from P5 neurons show high rates of spontaneous synaptic activity. Scale bars: **A-B.** 25 μm; **C.** 100pA by 100 msec.

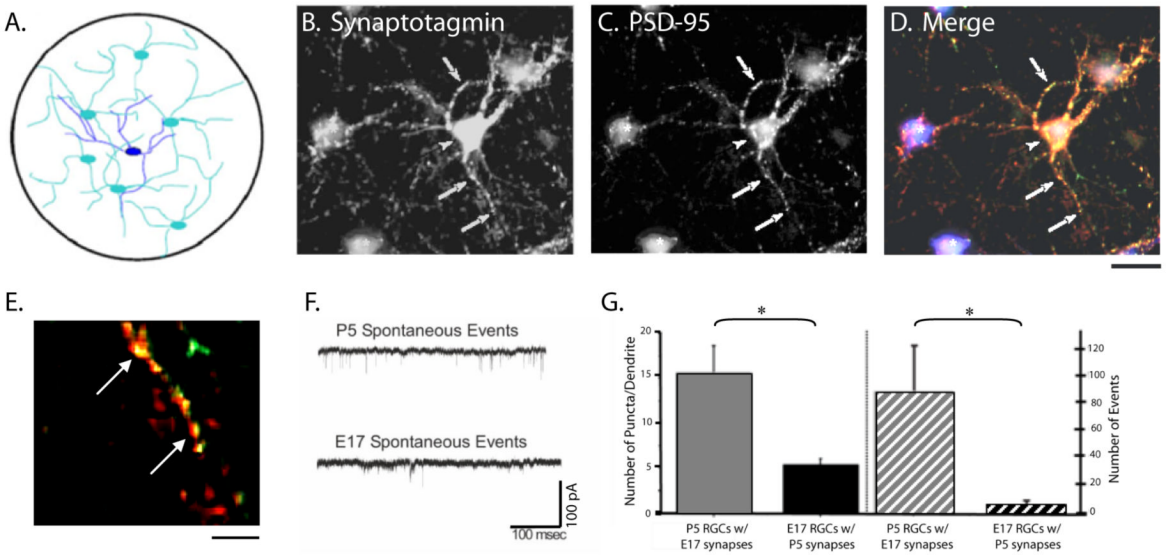

Figure 2.

Heterochronic co-cultures of labeled P5 neurons and E17 neurons. **A.** Example of the culture technique: labeled P5 neurons (dark blue) are co-cultured with unlabeled E17 neurons (turquoise) allowing for identification of the postnatal population. **B.-D.** P5 neuron (arrow head) co-cultured with E17 neurons (asterisks) and labeled for synaptotagmin (red; **B**) and PSD-95 (green; **C**). **D.** The P5 neuron shows more synaptic staining and a greater colocalization of pre and postsynaptic markers (arrows) than E17 neurons. **E.** High magnification of P5 dendrite shown in (**D**) shows numerous synaptic puncta (yellow; arrows). **F.** Spontaneous activity recorded with whole-cell patch-clamp from P5 neurons shows numerous synaptic events (downward deflections, top). In contrast recordings made from E17 neurons show fewer spontaneous synaptic events (bottom). **G.** Quantification of synaptic puncta per dendrite on E17 and P5 neurons in heterochronic culture conditions reveals a three-fold increase in the number of synapses on P5 neurons compared to E17 neurons. ($p < 0.001$, t-test). (left) Quantification of the number of synaptic events shows a nearly 10-fold increase in the number of spontaneous events/minute recorded from P5 neurons with synapses from E17 neurons compared to synaptic events recorded from E17 neurons with synapses from P5 neurons. (right) Scale bars: **B-D.** 50 μm; **E.** 10μm; **F.** 100 pA by 100 msec.

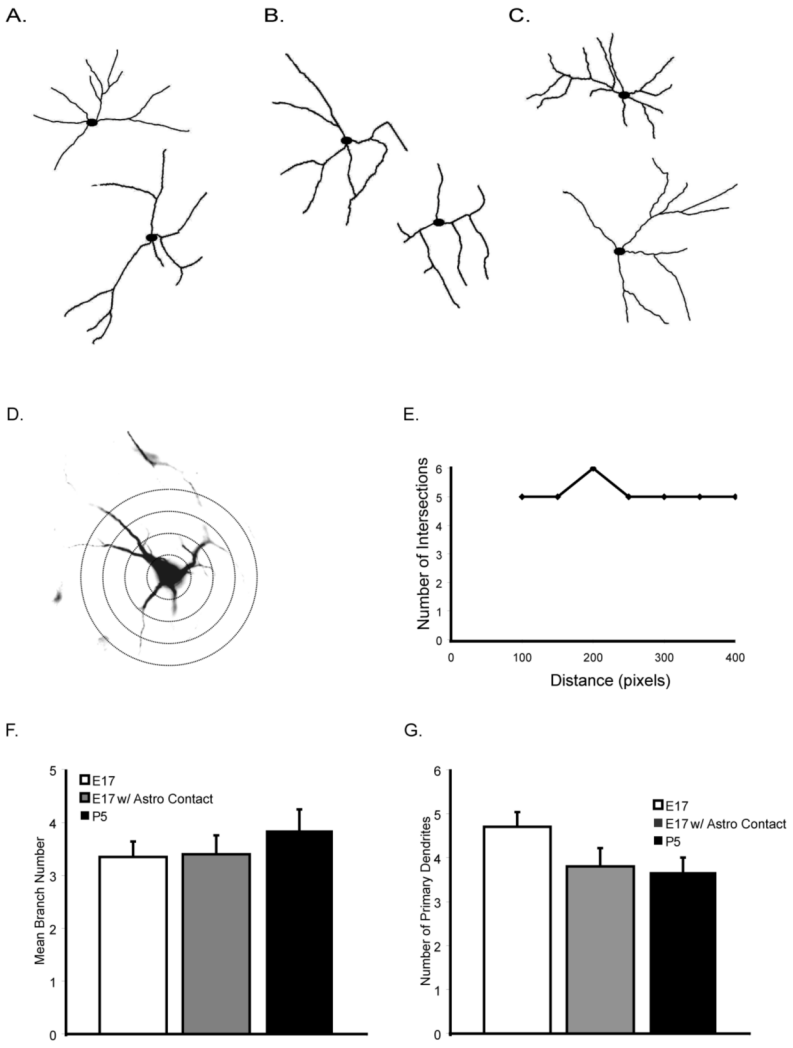

Figure 3.

E17 and P5 neurons exhibit equivalent dendrite elaboration as illustrated by representative traces. **A.** E17 RGCs. **B.** E17 RGCs with direct astrocyte contact **C.** P5 RGCs. **D.** Sholl analysis was used to quantify dendritic complexity. **E.** Representative Sholl analysis for neuron shown in (**D**). **F.** Sholl analysis was further used to quantify mean dendritic branch number. **G.** Number of primary dendrites was also analyzed using Sholl analysis. No statistically significant difference was found between all three conditions.

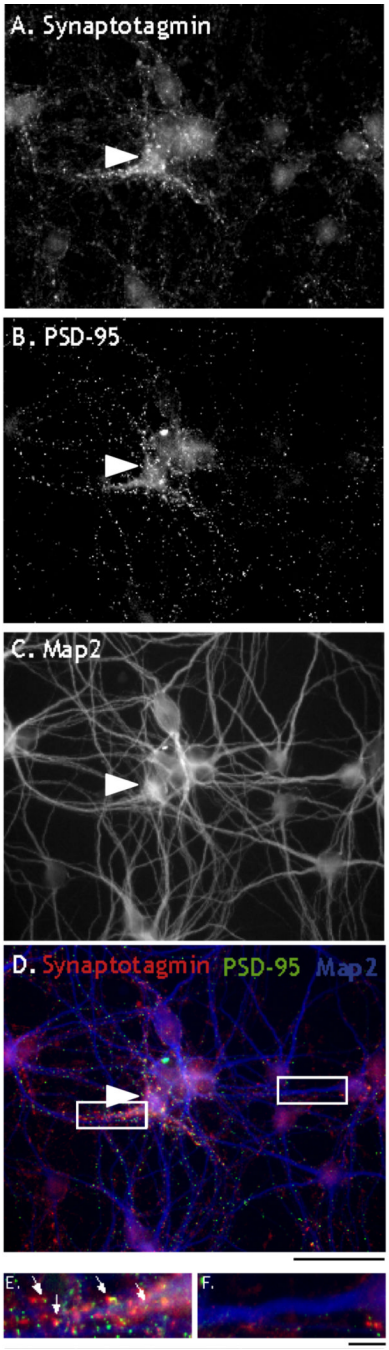

Figure 4.

E17 neurons do not receive many synapses despite the presence of elongated dendrites in heterochronic cultures. **A-B.** Heterochronic E17 and P5 neuron culture stained for presynaptic marker, Synaptotagmin (**A**) and postsynaptic marker, PSD-95 (**B**) Most synaptic puncta are associated with the P5 neuron (arrow head) Few puncta are visibly associated with E17 neurons. **C.** Dendritic staining shown in the same field as (**A-B**). Both P5 and E17 neurons contain numerous dendrites. **D.** Triple label of presynaptic marker synaptotagmin (red), postsynaptic marker PSD-95 (green), and dendritic marker MAP-2 (blue). Most colocalized puncta are found on P5 dendrites. **E**. Detail of synaptic staining along dendrite of P5 neuron showing colocalization of pre and postsynaptic markers (arrows). **F**. Detail of synaptic staining along

E17 dendrite. Few colocalized synaptic puncta are visible along the dendrite. Scale bars: **A-D.** 50μm; **E-F.** 10μm.

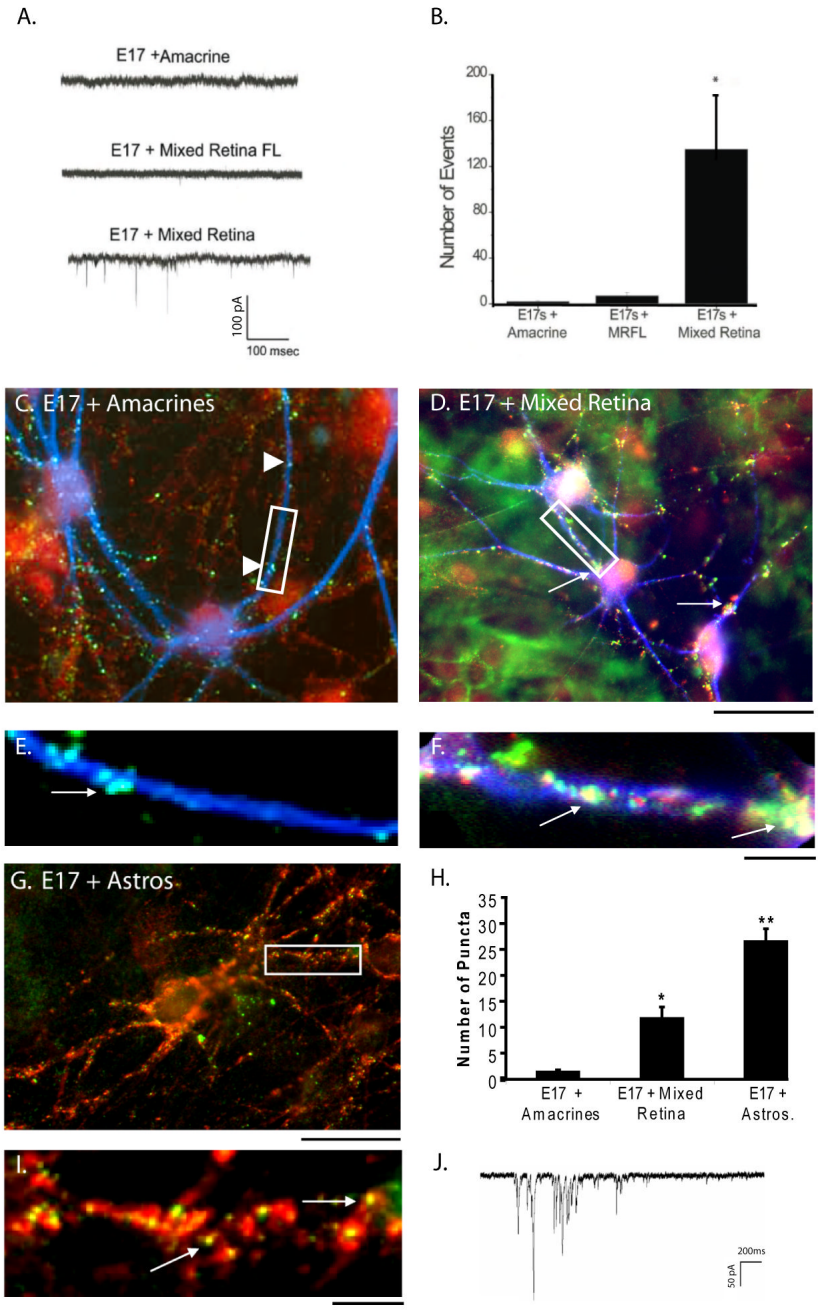

Figure 5.

Mixed retinal cells, but not purified amacrine cells, increase spontaneous synaptic activity and synapse number on E17 neurons. **A.** Patch-clamp recordings from E17 RGCs show few spontaneous events in neurons co-cultured with amacrine cells (top), but numerous synaptic events in neurons co-cultured with mixed retinal cells (bottom). E17 neurons cultured beneath mixed retinal feeding layers (Mixed Retina FL) also exhibit few spontaneous events (middle). **B.** Quantification of spontaneous events reveals over a 100-fold increase in synaptic events for neurons cultured with mixed retina compared to amacrine cells. **C.** Immunostaining for synaptic puncta (arrow heads) with synaptotagmin (red) and PSD-95 (green) shows few colocalized puncta on E17 neurons co-cultured with amacrine cells. Dendrites are stained with MAP-2 (blue). **D.** Increased number of synaptic puncta (arrows) is observed on E17 neurons

co-cultured with mixed retina. Dendrites are stained with MAP-2 (blue) Neurons are plated on top of a confluent layer of mixed retinal cells. **E.** Detail of synaptic staining as shown in (**C**). Few co-localized puncta are visible along the dendrite. **F.** Detail of synaptic staining as shown in (**D**). Increases in co-localized puncta are observed. **G.** E17 neurons cultured in contact with astrocytes show an increase in the number of colocalized synaptic puncta stained for synaptotagmin (red) and PSD-95 (green). Neurons are plated on top of a confluent monolayer of astrocytes. **H.** Quantification of synaptic puncta reveals a 9-fold increase in puncta when E17 RGCs are cultured on mixed retinal cells when compared to amacrines and a 19-fold increase when cultured on astrocytes compared to amacrines. **I.** High power image of colocalized puncta (arrows) on E17 neurons with astrocyte contact. **J.** E17 neurons co-cultured with astrocytes show marked increases in spontaneous synaptic currents as measured by whole-cell patch-clamp recording. Scale bars: **A.** 100pA by 100 msec; **C-D, G.** 50μm; **E.-F, I.** 10μm; **J.** 50pA by 200msec.

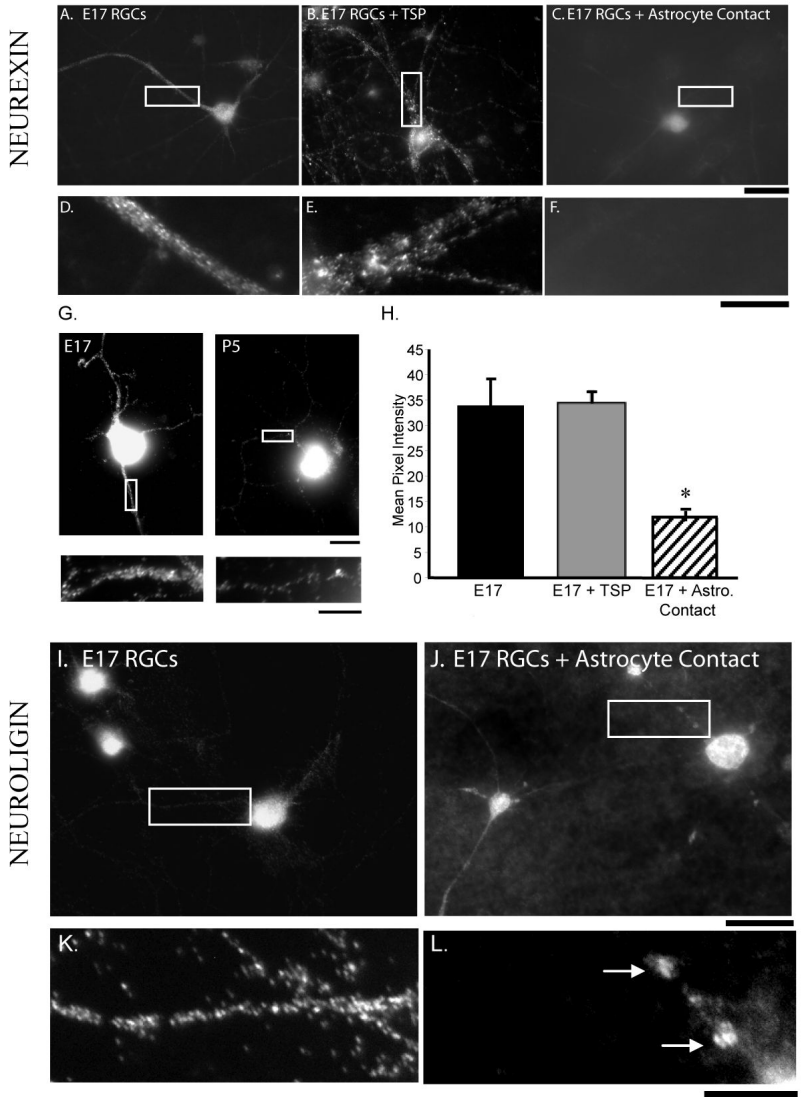

Figure 6.

Astrocyte contact induces changes in localization and intensity of the synaptic proteins neurexin and neuroligin in E17 RGCs. **A.** Neurexin staining of E17 RGCs cultured without astrocyte contact. **B.** Neurexin staining of E17 RGCs treated with TSP. **C.** Neurexin staining of E17 RGCs in contact with astrocytes. Intensity of neurexin staining decreases in E17 RGC dendrites when cultured on astrocytes, but not with TSP treatment. **D.** Detail of neurexin staining shown in (**A**). **E.** Detail of neurexin staining shown in (**B**). **F.** Detail of neurexin staining shown in (**C**). Quantification shows a significant decrease in intensity of neurexin staining (**H.**). **G.** Intensity of dendritic neurexin localization decreases in P5 RGCs when compared to E17 RGCs. Neurexin staining in E17 RGCs and high magnification of dendrite (left). Neurexin staining in P5 RGCs and high magnification of dendrite (right). **H.** Quantification of the intensity of neurexin staining shows a significant reduction when E17 RGCs are cultured in direct contact with astrocytes, but under conditions of TSP treatment. **I.** E17 RGCs cultured without astrocyte contact exhibit diffuse neuroligin staining along dendrites. **J**. When cultured in contact with astrocytes neuroligin staining becomes punctate along dendrites. **K.** Detail of neuroligin staining shown in (**I**). **L.** Detail of neuroligin staining

in E17 RGCs on astrocytes shown in (**J**), showing large puncta (arrows). Scale bars: **A-C, I-J** 50μm; **D-G, K-L** 10μm.

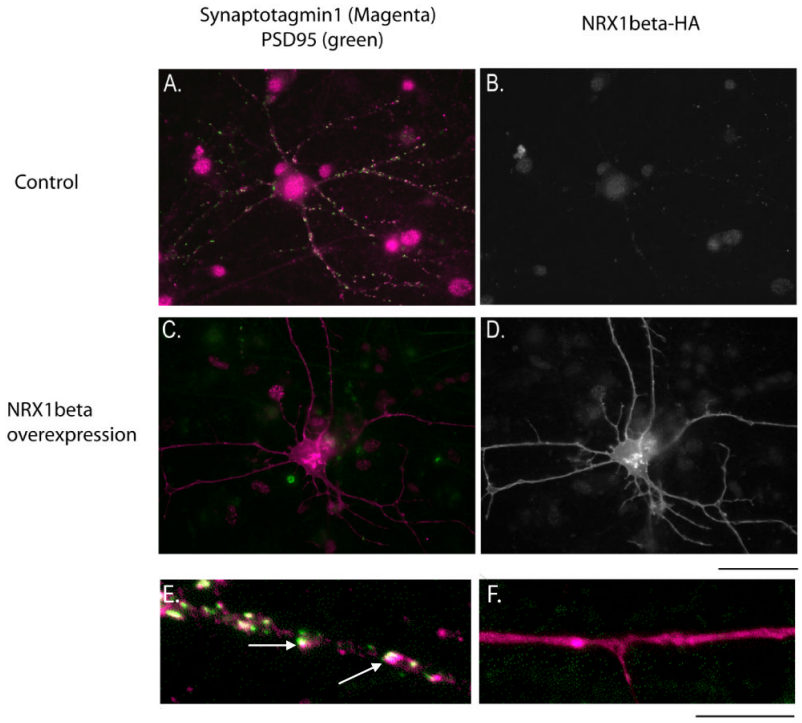

Figure 7.

Overexpression of NRX1β greatly reduces the synapogenetic effects of astrocyte contact on embryonic RGCs. Embryonic neurons are plated on top of a confluent monolayer of astrocytes. **A.** E17 RGCs co-cultured with astrocytes exhibit many synaptic puncta. **C.** E17 RGCs co-cultured with astrocytes and transfected with an HA-tagged NRX1β construct exhibit few synapses. **B, D.** Transfection of the HA-tagged NRX1β construct is visualized by staining for the HA tag. High magnification images of untransfected E17 RGCs (**E.**) and NRX1β transfected E17 RGCs (**F.**) highlight the large reduction in synapse number when NRX1β is overexpressed (synaptic puncta denoted by arrows). Quantification of synapse number reveals a highly significant reduction ($p < 0.000005$, student's t-test). Scale bars: **A**-**D**. 50 μm; **E**-**F.** 10 μm.